FABAD J. Pharm. Sci., 48, 1, 37-52, 2023
Doi: 10.55262/fabadeczacilik.1145208
RESEARCH ARTICLE

Ifosfamide-Loaded Cubosomes: An Approach to Potentiate Cytotoxicity against MDA-MB-231 Breast Cancer Cells

Popat S. KUMBHAR[*°] , Vishvajit M. KHADE[**], Varsha S. KHADAKE[***], Pradnya S. MARALE[****], Arehalli S. MANJAPPA[*****], Sameer J. NADAF[******], Vijay M. KUMBAR[*******], Durgacharan A. BHAGWAT[********], Ravindra A. MARATHE[*********], John I. DISOUZA[**********°]

Ifosfamide-Loaded Cubosomes: An Approach to Potentiate Cytotoxicity against MDA-MB-231 Breast Cancer Cells

SUMMARY

Ifosfamide (IFS) is proven efficacious against breast cancer, an enormously diagnosed cancer across the globe. However, the clinical efficacy of IFS is limited owing to its hydrophilicity, less stability, and dose-dependent toxicities. Therefore, the primary goal of the present research was to develop IFS-loaded cubosomes with improved anticancer efficacy and reduced dose-dependent toxicities. The IFS-cubosomes were optimized using a 32factorial design based on IFS content and zeta potential. The optimized cubosomal dispersion was further assessed for particle size, in vitro IFS release, hemolysis, cytotoxicity, cellular uptake, and physical stability. The optimized IFS-cubosomal dispersion exhibited maximum IFS content (89.75±4.3%) and better zeta potential value (-40.0±1.6 mV), and size in nanometer. Moreover, IFS-cubosomes retarded IFS release (about 91 %) 12 h than plain IFS solution (>99 % within 2 h). The IFS-cubosomes displayed lower hemolysis (3.7±0.79%) towards human RBCs. Besides, the in vitro cytotoxicity of IFS-cubosomes was noticed to be substantially higher (IC50: 0.64±0.08 µM) than plain IFS solution (IC50: 1.46±0.21 µM) against multi-drug resistant (MDR) breast cancer (MDA-MB-231) cells. The 4',6-diamidino-2-phenylindole (DAPI) staining revealed the death of IFS-cubosomes treated cells mainly by apoptosis. The cubosomes showed increased uptake by cancer cells. Furthermore, IFS-cubosomes were found to be more stable at refrigeration temperature than at room temperature. Thus, IFS-cubosomes could be a novel avenue in the treatment of breast cancer with improved anticancer efficacy and reduced toxicity. However, further in vivo investigations are desired to validate these claims.

Key Words: *Breast cancer, ifosfamide, cubosomes, haemolysis, cytotoxicity, cellular uptake.*

İfosfamid Yüklü Kübozomlar: MDA-MB-231 Meme Kanseri Hücrelerine Karşı Sitotoksisiteyi Güçlendirmeye Yönelik Bir Yaklaşım

ÖZ

İfosfamidin (IFS), dünya çapında çok fazla teşhis edilen bir kanser olan meme kanserine karşı etkili olduğu kanıtlanmıştır. Bununla birlikte, hidrofilikliği, daha az stabilitesi ve doza bağlı toksisiteleri nedeniyle IFS'nin klinik etkinliği sınırlıdır. Bu nedenle, mevcut araştırmanın birincil amacı, gelişmiş antikanser etkinliği ve doza bağlı toksisiteleri azaltılmış IFS yüklü kübozomlar geliştirmektir. IFS-kübozomları, IFS içeriğine ve zeta potansiyeline dayalı 32 faktörlü bir tasarım kullanılarak optimize edildi. Optimize edilmiş kübozomal dispersiyon ayrıca partikül boyutu, in vitro IFS salımı, hemoliz, sitotoksisite, hücresel alım ve fiziksel stabilite açısından da değerlendirildi. Optimize edilmiş IFS-kübozomal dispersiyonu, maksimum IFS içeriği (%89.75±4.3) ve daha iyi zeta potansiyel değeri (-40.0±1.6 mV) ve nanometre cinsinden boyut sergiledi. Ayrıca , IFS-kübozomlar, IFS salımını (yaklaşık %91) düz- IFS solüsyonuna (2 saat içinde >%99) göre 12 saat geciktirmiştir. IFS-kübozomları, insan RBC'lerine karşı daha düşük hemoliz (%3.7±0.79) gösterdi. Ayrıca, IFS-kübozomların in vitro sitotoksisitesinin, çoklu ilaca dirençli (MDR) meme kanserine (MDA-MB--231 hücreler) karşı düz IFS solüsyonundan (IC50: 1.46±0.21 µM) önemli ölçüde daha yüksek (IC50: 0.64±0.08 µM) olduğu fark edildi. 4',6-diamidino-2-phenylindole(DAPI) boyaması, IFS-kübozomlarla tedavi edilen hücrelerin başlıca apoptoz yoluyla ölümünü ortaya çıkardı. Kübozomların kanser hücrelerine alımları yüksek düzeyde gerçekleşti. Ayrıca, IFS-kübozomlarının buzdolabı sıcaklığında oda sıcaklığından daha kararlı olduğu bulundu. Bu nedenlerle IFS-kübozomlar, gelişmiş antikanser etkinliği ve azaltılmış toksisitesi ile meme kanseri tedavisinde yeni bir yol olabilir. Bununla birlikte, bu iddiaları doğrulamak için daha fazla in vivo araştırma istenmektedir.

Anahtar Kelimeler: *Meme kanseri, ifosfamid, kübozomlar, hemoliz, sitotoksisite, hücresel alım.*

Received: 18.07.2022 *Revised: 01.10.2022* *Accepted: 17.10.2022*

[*] ORCID: 0000-0002-6753-239X, Tatyasaheb Kore College of Pharmacy, Warananagar, Tal: Panhala, Dist: Kolhapur Maharashtra, India, 416113
[**] ORCID: 0000-0002-7522-8400, Tatyasaheb Kore College of Pharmacy, Warananagar, Tal: Panhala, Dist: Kolhapur Maharashtra, India, 416113
[***] ORCID: 0000-0003-3623-6595, Tatyasaheb Kore College of Pharmacy, Warananagar, Tal: Panhala, Dist: Kolhapur Maharashtra, India, 416113
[****] ORCID: 0000-0003-2633-5928, Tatyasaheb Kore College of Pharmacy, Warananagar, Tal: Panhala, Dist: Kolhapur Maharashtra, India, 416113
[*****] ORCID: 0000-0002-8576-6608, Tatyasaheb Kore College of Pharmacy, Warananagar, Tal: Panhala, Dist: Kolhapur Maharashtra, India, 416113
[******] ORCID: 0000-0002-7132-1886, Sant Gajanan Maharaj College of Pharmacy, Mahagaon, Gadhinglaj, Maharashtra, India
[*******] ORCID: 0000-0001-6261-1665, Dr. Prabhakar Kore Basic Science Research Centre, KLE Academy of Higher Education & Research, Belagavi, India
[********] ORCID: 0000-0002-3993-8851, Bharati Vidyapeeth College of Pharmacy, Kolhapur 416013, Maharashtra, India
[*********] ORCID: 0000-0002-9807-7932, Tatyasaheb Kore College of Pharmacy, Warananagar, Tal: Panhala, Dist: Kolhapur Maharashtra, India, 416113
[**********] ORCID: 0000-0002-0180-7266, Bharati Vidyapeeth (Deemed to be University), Yashwantrao Mohite Institute of Management, Karad

[°] Corresponding Author;
1. Dr. John I. Disouza
Phone: 02328 223526, Fax: 02328 223501
Email: jidisouza@tkcpwarana.ac.in

2. Mr. Popat S. Kumbhar
Phone: 02328 223526, Fax: 02328 223501
Email: pskumbhar@tkcpwarana.ac.in

INTRODUCTION

Cancer is the second most common cause of mortality globally. Amongst the various cancers, female breast cancer is the most prevalent cancer with a diagnosis rate of 11.7% followed by lung cancer (11.4%). Breast cancer is conceivably the single most important medical condition women face at present. It is an unrestrained growth of epithelial cells in the ducts or breast lobules (Elakkad, 2021). Breast cancer, from etiology to cure, is a complex disease that needs multidisciplinary management including a customized therapy plan based on severity and histologic subtype (Rick, 2021).

So far, surgery and chemotherapy are preferred procedures for the treatment of breast cancer either alone or in combination (Almotwaa, 2021). However, chemotherapy is associated with numerous side effects including myelosuppression, neurotoxicity, gastrointestinal dysfunctions, and damage to enteric neurons (Carr, 2008; McQuade, 2016; Escalante, 2017), *etc*. Furthermore, adverse effects of chemotherapy are identified to disturb the psychological health of patients and thereby impact their quality of life and social interactions (Suwankhong, 2018).

Ifosfamide (IFS) is a DNA alkylating therapeutic employed in the treatment of diverse cancers including lung, ovary, cervix, breast, and endometrium cancer (Wang, 2018; Almotwaa, 2021).It mainly acts *via* inhibition of DNA replication and thereby causes cell apoptosis. Nevertheless, the clinical efficacy of IFS is limited owing to its hydrophilic characteristics and dose-related toxicities such as encephalopathy, neurotoxicity, nephrotoxicity, and cardiotoxicity (Almotwaa, 2021).Hemorrhagic cystitis is a dose-limiting toxicity of IFS (Saito, 2016). Further, pH-dependent solubility profiling (Wang, 2018), multi-drug resistance (MDR) (Zhang, 2010; Noujaim, 2018),*etc.* are the other parameters that limit its therapeutic efficacy. Thus, to overcome the above issues, there is an utmost need to develop a suitable nanocarrier to deliver IFS with increased bioavailability, selectivity and stability with decreased side effects and MDR.

Lipid-based nanosized systems, for example, solid-lipid nanoparticles, nanostructured-lipid carriers, liposomes, cubosomes, hexosomes, *etc*., have revolutionized cancer management *via* improving anti-cancer effects of ample therapeutic actives (Garcia-Pinel, 2019). Cubosomes are cubic liquid crystalline particles that are a surfactant of self-assembled liquid crystalline particles with the right microstructure/nanostructure and water ratio. Cubosomes offer numerous formulation benefits including high encapsulation capacity, delivery of hydrophilic, hydrophobic, and amphiphilic drugs, biodegradability, biocompatibility, and increased physical and chemical stabilization of drugs (Lakshmi, 2014). In addition, cubosomes can be administered *via* various routes (oral, topical, and intravenous) of administration.

Both cubosomes and liposomes were reported to exhibit an increase in pharmacokinetic and pharmacodynamic results to intravenous administration that can broaden the therapeutic window and results in the enhancement of therapeutic efficacy. Besides, they were found to be promising in the reduction of neurotoxicity, cardiotoxicity, nephrotoxicity, ototoxicity, hepatotoxicity, and hematological toxicities (Alavi, 2020). For instance, the delivery of doxorubicin *via* liposomes caused a reduction of cardiotoxicity and other types of toxicities associated with doxorubicin (Addeo, 2008). Furthermore, cubosomes were reported to minimize the MDR in the treatment of cancer (Alavi, 2020). Cubosomes can also selectively target cancer cells *via* the enhanced permeation and retention (EPR) effect.

Glycerol monooleate (GMO) is a commonly employed lipid in the fabrication of cubosomes. GMO in the presence of excess water form liquid crystalline cubic phases that can control the release of the drug molecules. Moreover, it can deliver therapeutics of varying molecular sizes and solubilities (Nasr, 2015).

The main intend of the present research was to develop IFS-loaded cubosomes with improved cytotoxicity towards cancer cells, increased stability and reduced toxicities. The cubosomes were optimized using an experimental design approach and the optimized formulation was subjected to different *in vitro* analysis.

MATERIALS AND METHODS

MATERIALS

Ifosfamide was purchased from Believe Pharma, Gujarat. Glyceryl monooleate and Poloxamer-188 (P-188) were procured from Sigma Aldrich, Mumbai. Methanol and chloroform were obtained from Molychem, Mumbai. All the analytical grade chemicals were used in the experiments.

METHODS

Preparation of IFS-loaded cubosomes

Briefly, GMO and P-188 have melted at 70±2°Cin a water bath. The weighed quantity of IFS was then dissolved into double-distilled water maintained at 70±2°C with stirring. Then the melted mixture was gradually added to the double-distilled with the aid of stirring. The obtained dispersion was then subjected to probe sonication for 10 min employing an energy input (400 W) and a pulse mode (9-second pulses interrupted by 18-second breaks) under cooling in a 20°C water bath.

Optimization of IFS-loaded cubosomes

The IFS-loaded cubosomes formulation was optimized using 3^2 (2-factor, 3-levels) factorial design *via* Design-Expert software Version 13.0 (Stat-Ease Inc., Minneapolis, USA). Total of 09 runs (F1-F9) were generated using software and the consequence of independent variables was investigated on response variables at three levels. GMO concentration (X_1) and P-188 concentration (X_2) were selected as independent variables, whereas drug content (Y_1), and zeta potential (Y_2) as dependent variables. All independent and response variables with their coded and actual levels are shown in Table 1. Experimental runs were prepared according to the software-generated experimental design matrix (Table 2) and evaluated for results. The statistical significance of obtained results was evaluated by analysis of variance (ANOVA). 3-D response surface and 2-D contour plots were also obtained *via* design expert software and the consequence of independent variables on dependent variables were investigated further.

Table 1. Independent and dependent variables used with their coded and actual levels

Variables	Levels		
	Low (-1)	Medium (0)	High (+1)
Independent variables			
X_1: GMO concentration (mg)	0.25	0.5	1
X_2: Poloxamer concentration (mg)	0.5	1	1.5
Dependent (response) variables	**Goal**		
Y_1: Drug content (%)	Maximize		
Y_2: Zeta potential (mV)	Maximize		

Characterization of IFS-loaded cubosomes

% Entrapment efficiency (%EE)

Cubosome formulation was centrifuged at 10000 rpm for 1hand the clear supernatant was collected. The free IFS content in the supernatant was estimated *via* a UV-visible spectrophotometer at 249 nm after suitable dilution with methanol (Zhang, 2010; Siddiqui, 2019). The maximum wavelength of IFS obtained in methanol is depicted in Figure 1. The %EE of cubosome formulation was determined using the following formula (1);

$$\%EE = \frac{Tp - Tf}{Tp} \times 100 \quad (1)$$

Where Tp is the total IFS used to prepare the cubosomes and Tf is the free IFS in the supernatant.

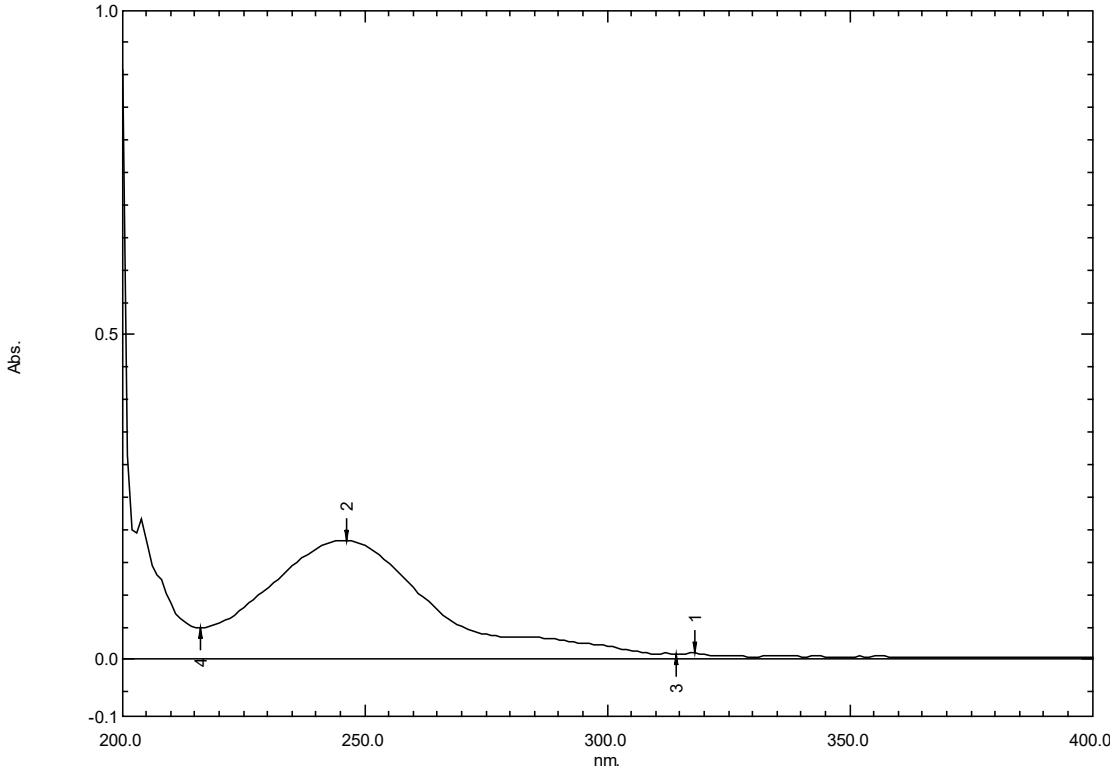

Figure 1. UV-spectra of ifosfamide in methanol

Vesicle size and Zeta potential

The particle size of the optimized batch and blank cubosomes, and zeta potential of all the formulated batches of IFS-loaded cubosomes were investigated using a Zeta sizer (Nano ZS, Malvern, UK).The samples (1 mL) were analyzed in triplicate at 25 ± 0.5°C following dilution with deionized water (29 mL) (Noujaim, 2018).

***In vitro* release**

The dialysis bag technique was employed to assess *in vitro* release behaviour of IFS from cubosomes and was compared with plain IFS solution. Briefly, both optimized IFS cubosomes (equivalent to 2 mg IFS) and plain IFS (2 mg) solution were filled in a separate dialysis bag (Molecular weight cut-off 12000). The dialysis bag was then immersed in 50 mL of release medium (phosphate buffer saline; PBS pH 6.8.) controlled at 37±2°C and 150 rpm. The release medium (2 mL) was collected following a determined time interval and the equivalent volume was substituted with fresh PBS pH 6.8. The collected solutions were assessed by UV-visible spectrophotometer at 249 nm. The experiment was repeated three times and the% cumulative IFS release from cubosomes and the plain solution was calculated (Nasr, 2015; Nasri, 2020).

***In vitro* hemolysis**

In vitro hemolysis of optimized IFS-cubosomes was carried out using human blood to investigate its safety and compatibility for intravenous use. The defibrinogeneted blood (3 mL) was diluted using 0.9% sodium chloride solution (10mL) and allowed to centrifuge at 1000rpm for 10 minutes to obtain erythrocyte pellets. The resultant pellet was washed repeatedly (3-4 times) using 0.9% NaCl solution and subsequently diluted with the same solution to obtain 3% erythrocyte dispersion which was set aside at 4°C until further use. The IFS-cubosomes were introduced into flasks holding 1mL of 3% erythrocyte dispersion and

the ultimate volume was attuned to 5mL with 0.9% NaCl solution to achieve a final concentration of 50 **µg/mL** respectively. A similar experiment was carried out with a plain IFS solution to achieve a concentration of 50 µg/mL respectively. 1mL of erythrocyte dispersion with 4mL 0.9% NaCl solution was considered a negative control whereas 1mL dispersion containing 4mL of deionized water was a positive control. All the aforementioned dispersions were incubated for 2h at 37±2°C. Following incubation, the dispersions were centrifuged (5000rpm) for 10 minutes. Resultant pellets were collected, re-dispersed in deionized water, and sonicated for 5 minutes. Next, the system was centrifuged (10000rpm) for 10 minutes and the absorbance of the supernatant was recorded at 420nm with a UV-visible spectrophotometer against deionized water as blank. The % hemolysis was computed *via* the following formula (Sambamoorthy, 2021).

$$\%Hemolysis = \frac{Test\ sample\ absorbance - Negative\ control\ absorbance}{Positive\ control\ absorbance - Negative\ control\ absorbance} \quad (2)$$

***In vitro* cytotoxicity**

The consequence of plain IFS and optimized IFS-cubosomes on the viability of breast cancer-resistant (MDA-MB 231) cells was investigated *via* a3-(4,5-dimethylthiazol-2-yl)-2,5-diphenyl-2H-tetrazolium bromide (MTT) dye reduction assay. Briefly, the cells were introduced to a 96-well plate and incubated overnight at 37°C and 5% CO_2. The cells were treated with the sample at diverse concentrations and plates were kept for another 48 h. Then 100µL of MTT (6 mg/10mL of MTT in PBS) was added to the plates by removing test solutions and the plates were further incubated for 4 h in an analogous environment. Eventually, the supernatant was eliminated and formazan crystals assembled in viable cells were solubilized by dimethyl sulphoxide (DMSO; 100µL). The absorbance of the ensuing solution was recorded at 570 nm employing a microplate. The IC_{50} values were then computed *via* dose-response curves (Kumbhar, 2020).

Apoptosis by (4', 6-diamidino-2-phenylindole) DAPI staining

The cells were seeded in a 24-well flat-bottom microplate containing a coverslip and controlled at 37°C in a CO_2incubator overnight. Next, cells were treated with IFS and IFS cubosomes at corresponding IC_{50} values and incubated for another 24 h. After the incubation, cells were washed with PBS and firmed with paraformaldehyde (4%) for 30 min. Finally, cells were contacted with DAPI (20 µL) for 5 minutes at room temperature in the dark and noticed under a fluorescent microscope (Bhat, 2018).

Cellular uptake study

Cells were introduced in 24 well plate holding coverslips and incubated overnight. Cells were then incubated with cubosomes (Rhodamine G-loaded) and incubated for 5 h, were firmed with paraformaldehyde (4%), and washed twice with PBS. Further, the nucleus cells were stained with DAPI. The cover slip containing the specimen was observed under the fluorescence microscope (Olympus BX41) (Andrgie, 2019).

***In vitro* stability**

The *in vitro* physical stability of cubosomes was assessed based on %EE and % cumulative drug release (%CDR) at different time intervals for three months of storage at refrigerator (2-8°C) and room temperature (25°C).

Statistical analysis

The statistical analysis was carried out *via* GraphPad Prism software version 8 (GraphPad Software, Inc., La Jolla, CA, USA). Data are depicted in terms of mean ± standard deviation independent experiments carried out in triplicate. The findings obtained were assessed through one-way and two-way ANOVA and statistically significant differences in the findings were expressed by considering $P<0.05$.

RESULTS AND DISCUSSION

Preparation of IFS-loaded cubosomes

The IFS-loaded cubosomal dispersions were prepared *via* rupturing a cubic gel phase composed of GMO and water withP-188 (stabilizer) by mechanical stirring. The formed cubosomal dispersions were uniform opaque white mixtures with an absence of aggregate.

Optimization of IFS-loaded cubosomes

Fitting of data to the model

The consequence of independent variables on dependent variables was thoroughly investigated using 3^2 factorial design. Total of 09 runs were generated and evaluated and results are reported in Table 2. All responses fitted to different models i.e. linear, two-factor interaction (2FI), and quadratic models. The best fit model was decided based on a high R^2 value and low predicted residual error sum of squares (PRESS). Best-fitted model for responses Y_1 and Y_2 was two-factor interactions (R^2: 0.9996 and PRESS: 2.35) and quadratic model (R^2: 0.9924 and PRESS: 5.05) respectively. This corroborates that suggested models can significantly predict the >99% variations in responses studied. The significance and efficacy of models were assessed by ANOVA. The Prob (p) value < 0.05 affirms the model term was significant. Model F- value for response variables Y_1 and Y_2 was found to be 4717.73 and 78.47 respectively, which indicates the significance of the model. For response Y_1, X_1, X_2, and X_1X_2 were significant model terms while, for Y_2, two factor terms [X_1 and X_2] and one quadratic term [X_1^2] were significant. For both responses, the predicted R^2 values of 0.9976 (Y_1) and 0.9456 (Y_2) were in agreement with adjusted R^2 of 0.9994 (Y_1) and 0.9798 (Y_2) respectively. Adequate precision values were found to be 202.90(Y_1) and 24.16 (Y_2). In general, a value greater than 4 is desired. Additionally, the multicollinearity of the formulation variables was evaluated based on the variance inflation factor (VIF). A VIF value of 1 reflected the absence of multicollinearity among the independent variables in the model.

The polynomial equation explaining the relationship between independent and dependent variables can be given as follows,

$$Y_1 \text{ (Drug content)} = +70.29 +7.36\, X_1 +10.49\, X_2 +1.45\, X_1 X_2 \quad (1)$$

$$Y_2 \text{ (Zeta potential)} = -42.38 +3.77\, X_1 +1.01 X_2 -0.0214 X_1 X_2 -2.09 X_1^2 -0.2500 X_2^2 \quad (2)$$

Factor coefficients from the polynomial equations were compared and the relative impact of the factors was assessed. In the case of both responses, the positive coefficient of X_1 and X_2 represents their synergistic effect on drug content and zeta potential. This means that drug content and zeta potential increased with an increase in the concentration of X_1 and X_2. The interaction term X_1X_2 showed a positive impact on drug content and a negative impact on zeta potential. Further, the F value of individual variables was compared to determine their impact on response. The F-value of 9308.94 confirmed the prominent effect of X_2 on drug content whereas, the F value of 362.36 indicated the prominent effect of X_1 on zeta potential. The 2-D contour (Figure 2A and 2C), and 3-D response surface plots (Figure 2B and 2D) confirmed the positive effects of independent variables on the response studied. Furthermore, the perturbation plots, where the response is determined by changing a single independent variable solely along its range, are helpful for interpreting the influence of independent factors on the response variables. The perturbation plots have also supported the same results (positive effects of independent variables on the response variables) obtained with 2-D and 3-D response surface plots. The steep slope for factor X_2 (Figure 3A) and curvature for X_1 (Figure 3B) confirmed their prominent effects on drug content and zeta potential respectively. The plots of predicted vs actual values for Y_1 and Y_2 are shown in Figure 3C and 3D. The

ANOVA results for both responses are summarized in Table 3 and model fit summary is presented in Table 4. Amongst the all batches prepared, batch F8 showing %EE of 89.75±4.3% and zeta potential of -40.0±1.6 mV (Figure 4A) was selected as an optimized batch. This optimized batch was further characterized for different parameters.

Table 2. Randomized experimental runs generated using 3^2 factorial design

Std	Run	X_1: GMO conc. (mg)	X_2: Poloxamer conc. (mg)	Y_1: Drug content (%)	Y_2: Zeta potential (mV)
6	1	1	1	77.25	-40.7
7	2	0.25	1.5	71.96	-47.3
3	3	1	0.5	65.96	-41.9
5	4	0.5	1	67.88	-43.4
2	5	0.5	0.5	57.67	-45.5
8	6	0.5	1.5	77.95	-43.2
1	7	0.25	0.5	54.07	-49.2
9	8	1	1.5	89.75	-40.0
4	9	0.25	1	62.76	-48.7

Table 3. ANOVA results for response Y_1 and Y_2

Source	Sum of Squares	Coeff	F-value	p-value
Response Y_1				
Model	985.84	70.29[a]	4717.73	< 0.0001[b]
A-GMO Conc.	337.25	7.36	4841.74	< 0.0001
B-Poloxamer Conc.	648.41	10.49	9308.94	< 0.0001
AB	8.75	1.45	125.61	< 0.0001
Residual	0.3483			
Cor Total	986.19			
Response Y_2				
Model	92.18	-42.38[a]	78.47	0.0022[b]
A-GMO Conc.	85.13	3.77	362.36	0.0003
B-Poloxamer Conc.	6.06	1.01	25.81	0.0147
AB	0.0019	-0.0214	0.0081	0.9339
A^2	6.64	-2.09	28.27	0.0130
B^2	0.1250	-0.2500	0.5321	0.5185
Residual	0.7048			
Cor Total	92.88			

[a]Intercept and [b] significant

Table 4. Model fit summary

Source	Sequential p-value	Lack of Fit p-value	Adjusted R^2	Predicted R^2	
Response Y_1					
Linear	< 0.0001		0.9877	0.9700	
2FI	**< 0.0001**		**0.9994**	**0.9976**	**Suggested**
Quadratic	0.4667		0.9994	0.9975	
Cubic	0.6316		0.9993	0.9782	**Aliased**
Response Y_2					
Linear	0.0005		0.8927	0.8531	
2FI	0.9729		0.8713	0.7422	
Quadratic	**0.0290**		**0.9798**	**0.9456**	**Suggested**
Cubic	0.9098		0.9498	-0.6157	**Aliased**

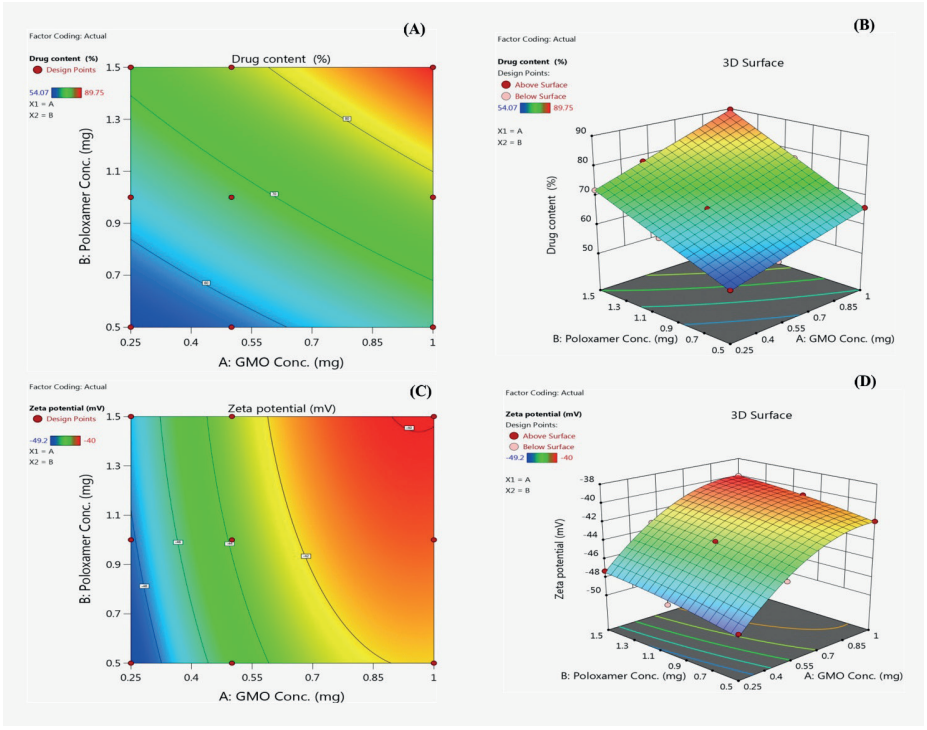

Figure 2. 2-D contour plots (2A and 2C) and 3-D response surface plots (2B and 2D) of independent variables showing effect on drug content and zeta potential

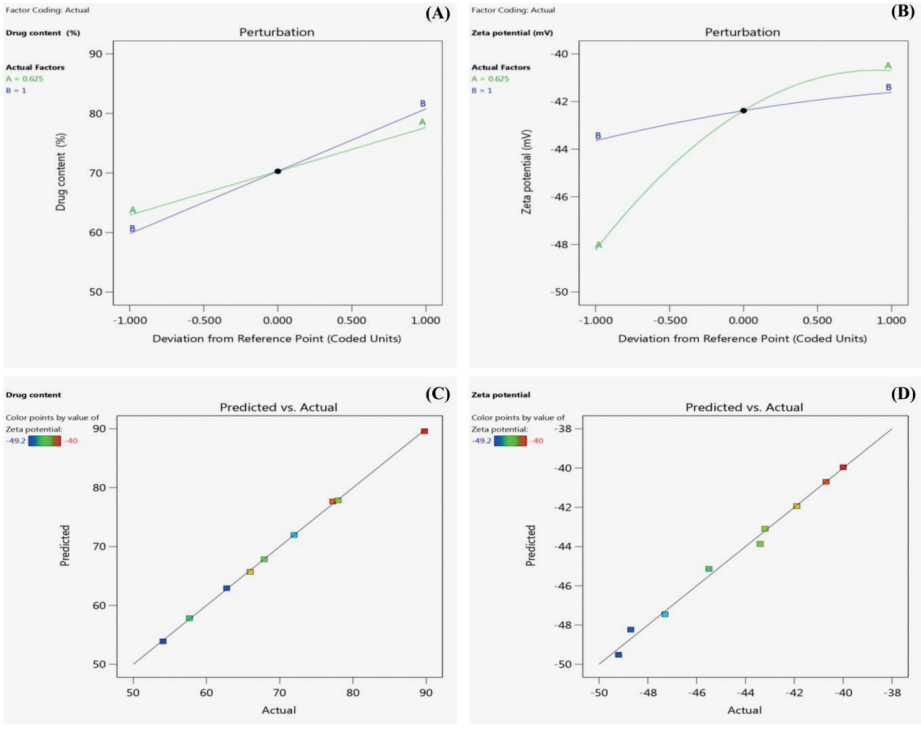

Figure 3. Perturbation plots **(A)** for factor X2 and **(B)** for factor X1, **(C & D)** predicted vs actual plot for Y1 and Y2

Particle size

The mean particle size of the optimized IFS-loaded cubosomes and blank cubosomes were found to be 192±7 nm (polydispersity index (PDI: 0.2±0.04) and 160±5 nm (PDI: 0.5±0.1) respectively (Figure 4B and 4C). This slight increase in the particle size of IFS-cubosomes is attributed to the loading of IFS in the cubosomes. The P-188 at high concentration might have contributed to form smaller and vesicular particles of cubosomes. These vesicular structures might be due to the development of bilayers amid mixed monoolein and poloxamer that cause sterically stabilization of the particles by evading their fusion into the cubic state (Gustafsson, 1996). Thus, the particle size of cubosomal dispersion was observed to be less than 200 nm which is essential to achieve targeting of IFS at the tumor *via* the EPR effect.

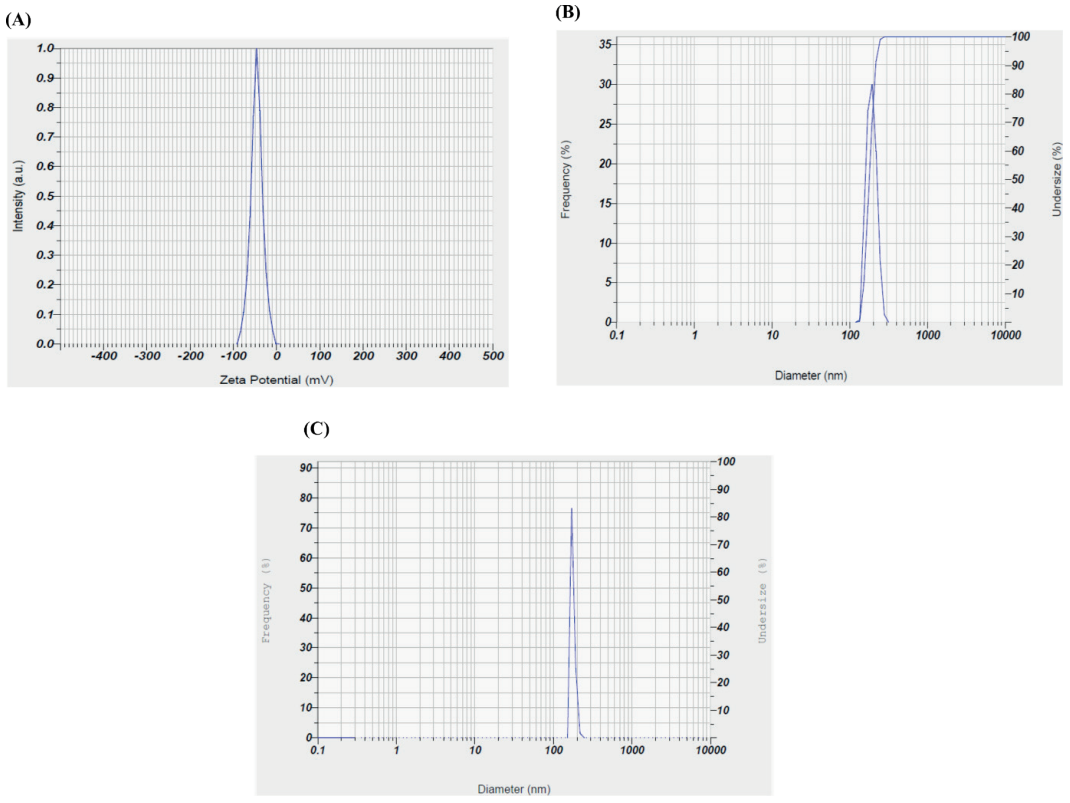

Figure 4. (A) Zeta potential of optimized cubosomes, **(B)** Mean particle size of optimized IFS-cubosomes, and **(C)** Blank cubosomes

***In vitro* drug release study**

The *in vitro* release of IFS from optimized cubosome was investigated *via* dialysis bag technique using PBS pH 6.8 and compared with plain IFS aqueous solution (Figure 5). IFS has displayed rapid and almost complete (99.54±7.5%) release from plain IFS (aqueous) solution within 2 h. In contrast, cubosomes have demonstrated a sustained release of IFS (91.12±7.22%) after 12 h. This remarkably slower release of IFS from the cubosomes could be due to the limited diffusion of IFS molecules entrapped in the aqueous channels of cubosomes where diffusion normally occurs *via* aqueous channels of narrow pore size. Thus, sustained release of IFS from cubosomes may retain the IFS in circulation for a longer time could cause better accumulation of drugs in the tumor *via* the EPR effect and, meet the criteria for an effective drug delivery carrier for cancer treatment (Nasr, 2015).

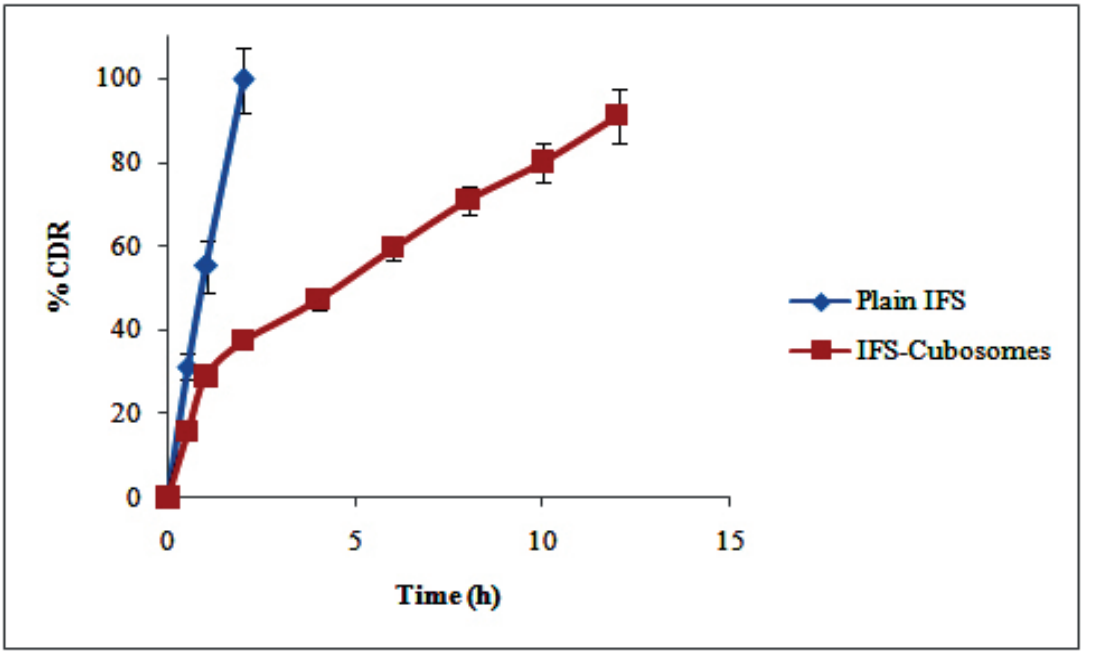

Figure 5. *In vitro* IFS release from plain IFS solution and IFS-cubosomes

***In vitro* hemolysis**

The compatibility of IFS and IFS cubosomal dispersion with the components of blood was assessed by *in vitro* hemolysis study. Herein, no hemoglobin was directly estimated to evade the interference of formulations that may alter the colour of hemoglobin. In the present research, the RBCs which remain intact following treatment with formulations were separated from the buoyant. The separated intact RBCs were lysed with deionized water and estimated for hemoglobin by subtracting its absorbance from the absorbance of positive control.

The plain IFS solution, blank cubosomes, and IFS-cubosomes have displayed % hemolysis of 2.6±0.23, 3.1±0.45, and 3.7±0.79%, respectively after 2 h of incubation. The slight increase in the hemolysis with cubosomes could be due to their interactions with blood components. However, no significant difference was observed in the % hemolysis with all three formulations. Thus, the lower hemolysis with IFS cubosomal dispersion indicates safety and appropriateness for intravenous injection (Sambamoorthy, 2021).

***In vitro* cytotoxicity**

The cytotoxic potential of plain IFS, blank cubosomes, and optimized IFS-cubosomes were investigated against breast cancer-resistant (MDA-MB-231) cells using an MTT dye reduction assay. Both plain IFS solution and IFS-cubosomes demonstrated cytotoxicity with respect to dose. The IFS-cubosomes have displayed substantially higher cytotoxicity (low IC_{50}: 0.64±0.08 µM) than plain IFS solution (IC_{50}: 1.46±0.21 µM) after 48 h of incubation. The blank cubosomes have shown very less cytotoxicity (11-23% inhibition of growth) after 48 h therefore IC_{50} value was not calculated.

The remarkable cytotoxicity of IFS-cubosomes could be due to the endocytosis-mediated cellular uptake in the tumor cell. In addition, the sustained release of IFS from the cubosomes may also be responsible for high cytotoxicity. Furthermore, poloxamer may cause an increase in the sensitivity of IFS toward MDR cells (Singh-Joy, 2008). Thus, obtained cytotoxicity results revealed that IFS was very efficient at a very low dose against cancer following its entrapment into the cubosomes. This reduction in

the dose of IFS can help to reduce the dose-dependent toxicities (neurotoxicity and nephrotoxicity and hemorrhagic cystitis) associated with IFS. Moreover, it can help to reduce MDR in the cancer cells especially breast cancer cell lines (Wang, 2018).

Apoptosis by DAPI staining

The alterations in the apoptotic nuclear morphology in MDA-MB-231 breast cancer cells were noticed after the treatment with IFS and IFS-cubosomes *via* DAPI staining. The normal intact nuclei with weak homogenous blue stains (Figure 6A) were noticed in the cells with no treatment. The IFS and IFS-cubosomes (Figure 6B and 6C) treated cells displayed small nuclei amidst blebbing, bright chromatin condensation, nuclear fragmentation, and generation of apoptotic bodies as shown in the picture. It was noticed that MDA-MB-231 cells treated with IFS-cubosomes demonstrated extreme fragmentation of the cell nuclei when compared to plain IFS. This extreme fragmentation of cell nuclei by IFS-cubosomes might be due to the increased cell accumulation and thereby higher cytotoxicity.

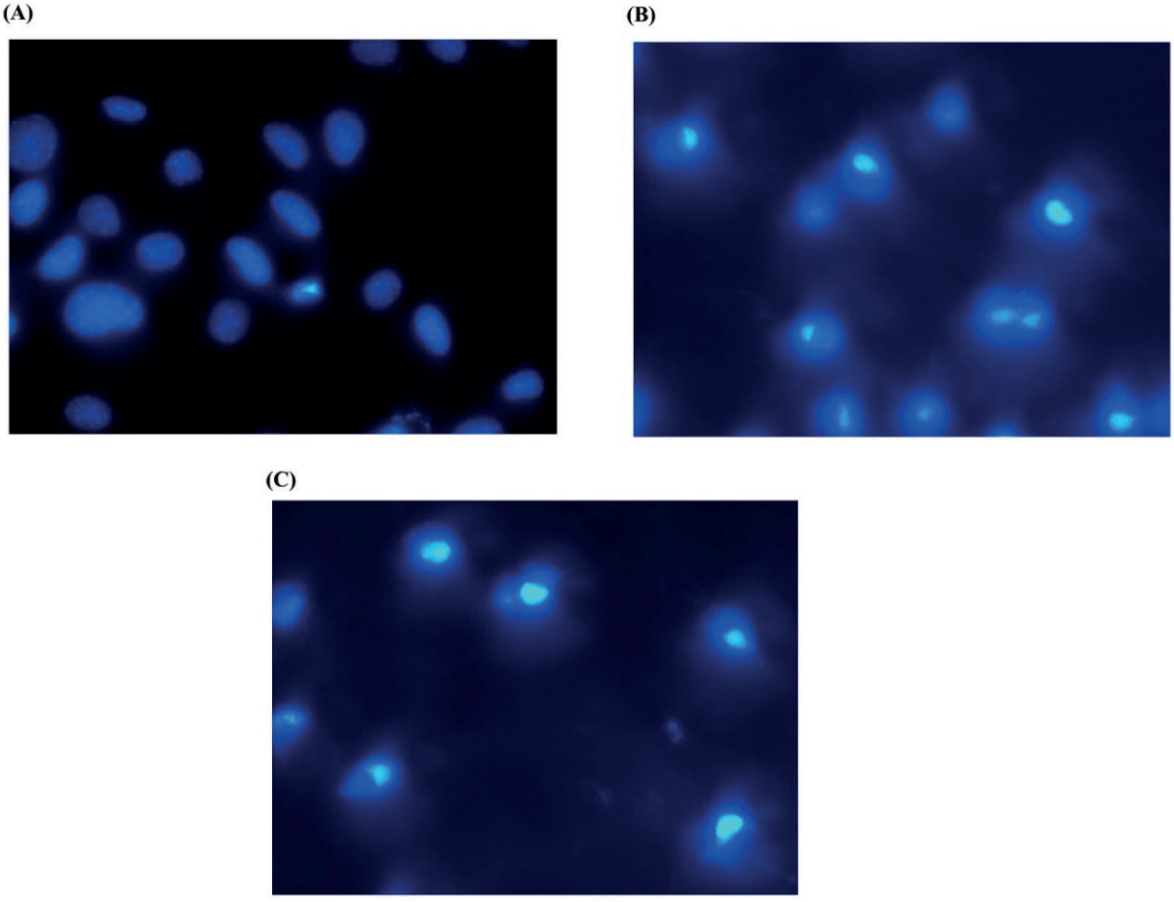

Figure 6. DAPI Apoptosis **(A)** Normal control, **(B)** Plain IFS treated and **(C)** IFS-cubosomes treated

Cellular uptake study

The cellular uptake potential of cubosomes was investigated using MDA-MB-231 cells. The cubosomes containing rhodamine G dye displayed intense red fluorescence indicating significant uptake of the cubosomes by the MDA-MB-231 cells (Figure 7A). Moreover, the nuclei of the cell were noticed to be blue owing to the DAPI stain (Figure 7B). The merged image showed blue stain nuclei of the cell and the presence of

rhodamine G-loaded cubosomes (Figure 7C). These obtained results confirmed the substantial uptake of IFS-cubosomes by the MDA-MB-231 cells. This increased uptake could be attributed to the nanosizing of prepared cubosomes that might have facilitated the physical interaction between the cubosomes and the cell membrane and thereby clustering of cubosomes on the cell surface and generation of cell membrane responses including disruption of permeability and integrity of cell membrane (Behzadi, 2017).

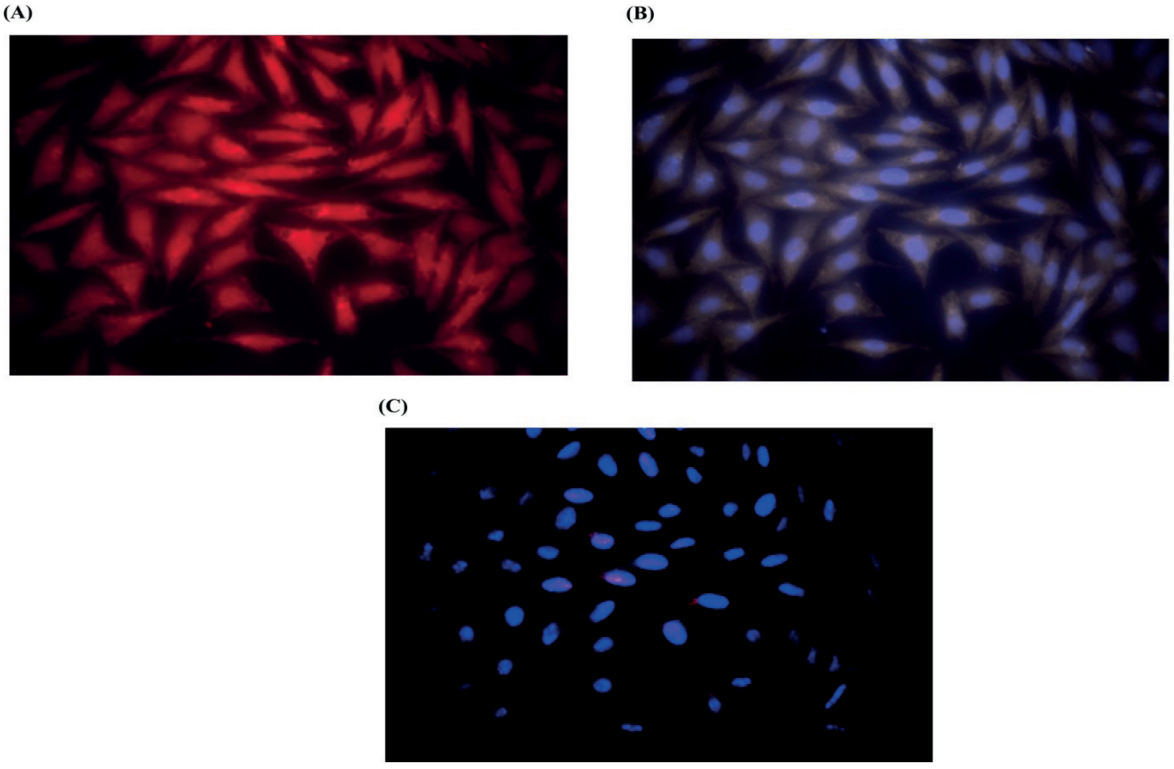

Figure 7. Cellular uptake **(A)** Rhodamine G-loaded cubosomes **(B)** DAPI stain in the nuclei of cell **(C)** Merged image of rhodamine G-loaded cubosomes and DAPI stained cell nuclei

Stability study

The *in vitro* (physical) stability of IFS-cubosomes was assessed based on the % EE and % CDR after storage at room temperature (25-30°C) and refrigerator (2-8°C) for three months (Table 5). No significant difference in the % EE and % CDR was observed following storage of cubosomes at refrigeration conditions indicating better stability of the IFS-cubosomes at refrigeration. In addition, no sign of phase separation was noticed. In contrast, during the storage at room temperature, % EE was reduced from 89 to 77% and % CDR from 91 to 70%. This could be attributed to the leakage of IFS from the cubosomes over time. This corroborates the poor storage stability of IFS-cubosomes at room temperature. Therefore, IFS-cubosomes could be stored safely in refrigeration conditions (Andrgie, 2019).

Table 5. Stability study optimized IFS-cubosomes at refrigerator condition and room temperature

Formulation	Storage condition	% EE				% CDR			
		Fresh	1 Month	2 Months	3 Months	Fresh	1 Month	2 Months	3 Months
IFS-cubosomes	Refrigerator temperature (2-8°C)	89.75±4.3	89.02±4.1	88.75±5.7	86.56±4.8	91.12±7.2	90.47±7.8	88.27±6.9	85.97±8.2
	Room temperature (25-30°C)	89.75±4.3	84.11±5.6	81.58±4.3	77.53±5.1	91.12±7.2	86.04±6.3	79.86±7.7	70.10±6.4

CONCLUSIONS

In the present research, the hydrophilic IFS-loaded cubosomes were successfully fabricated and optimized *via* factorial design. The IFS entrapment and zeta potential were found to be significantly dependent on the concentration of GMO and P-188. The optimized IFS-cubosomes displayed a size of less than 200 nm indicating their targeting potential at the site of the tumor *via* the EPR effect. Moreover, the release of IFS from IFS-cubosomes was noticed to be sustained, suggesting improved circulation and accumulation of IFS at the tumor. The IFS-cubosomes displayed lower hemolytic behavior revealing their biocompatibility and safety for intravenous injection. Furthermore, the remarkable cytotoxic potential of IFS-cubosomes at low dosage corroborates its enhanced anticancer effect without dose-dependent toxicities. In summary, cubosomes could serve as a carrier system to improve the anticancer potential of IFS at low doses and reduce toxicities. Nevertheless, *in vivo* testing's involving animal models are recommended to further ensure the formulation efficacy.

ACKNOWLEDGMENTS

We are greatly thankful to our Head of Institute and Institute Management for supporting this research project.

CONFLICT OF INTEREST

The authors declare that there is no conflict of interest.

AUTHOR CONTRIBUTION RATE STATEMENT

PK, VMK, VSK & PM: Performed all above research activities. PK & JD: Designed, monitored and coordinated the research activities. JD: Participated in statistical analysis and data interpretation. PK, SN, AM, VK, DB & RM: Involved in the preparation and drafting of the manuscript.

REFERENCES

Addeo, R., Faiola, V., Guarrasi, R., Montella, L., Vincenzi, B., Capasso, E., Cennamo, G., Rotundo, M. S., Tagliaferri, P., Caraglia, M., Del Prete, S. (2008). Liposomal pegylated doxorubicin plus vinorelbine combination as first-line chemotherapy for metastatic breast cancer in elderly women > or =65 years of age. *Cancer chemotherapy and pharmacology*, *62*(2), 285–292. https://doi.org/10.1007/s00280-007-0605-6.

Alavi, M., Webster, T. J. (2020). Nano liposomal and cubosomal formulations with platinum-based anticancer agents: therapeutic advances and challenges. *Nanomedicine (London, England)*, *15*(24), 2399–2410. https://doi.org/10.2217/nnm-2020-0199.

Almotwaa, Sahar. (2021). Coupling Ifosfamide to nanoemulsion-based clove oil enhances its toxicity on malignant breast cancer and cervical cancer cells. *Pharmacia*, 68. 779-787. http://dx.doi.org/10.3897/pharmacia.68.e68291

Andrgie, A. T., Birhan, Y. S., Mekonnen, T. W., Hanurry, E. Y., Darge, H. F., Lee, R. H., Chou, H. Y., Tsai, H. C. (2019). Redox-Responsive Heparin-Chlorambucil Conjugate Polymeric Prodrug for Improved Anti-Tumor Activity. *Polymers*, *12*(1), 43. https://doi.org/10.3390/polym12010043.

Behzadi, S., Serpooshan, V., Tao, W., Hamaly, M. A., Alkawareek, M. Y., Dreaden, E. C., Brown, D., Alkilany, A. M., Farokhzad, O. C., Mahmoudi, M. (2017). Cellular uptake of nanoparticles: journey inside the cell. *Chemical Society Reviews*, *46*(14), 4218–4244. https://doi.org/10.1039/c6cs00636a.

Bhat, S. S., Revankar, V. K., Kumbar, V., Bhat, K., Kawade, V. A. (2018). Synthesis, crystal structure and biological properties of a cis-dichloridobis(diimine)copper(II) complex. *Acta Crystallographica. Section C, Structural Chemistry*, *74*(Pt 2), 146–151. https://doi.org/10.1107/S2053229617018551.

Carr, C., Ng, J., Wigmore, T. (2008).The side effects of chemotherapeutic agents. *Current Anaesthesia Critical Care*, 19(2), 70–79.

Elakkad, Y. E., Mohamed, S., Abuelezz, N. Z. (2021). Potentiating the cytotoxic activity of a novel simvastatin-loaded cubosome against breast cancer cells: Insights on dual cell death via ferroptosis and apoptosis. *Breast Cancer (Dove Medical Press)*, *13*, 675–689. https://doi.org/10.2147/BCTT.S336712.

Escalante, J., McQuade, R. M., Stojanovska, V., Nurgali, K. (2017). Impact of chemotherapy on gastrointestinal functions and the enteric nervous system. *Maturitas*, *105*, 23–29. https://doi.org/10.1016/j.maturitas.2017.04.021

García-Pinel, B., Porras-Alcalá, C., Ortega-Rodríguez, A., Sarabia, F., Prados, J., Melguizo, C., López-Romero, J. M. (2019). Lipid-based nanoparticles: Application and recent advances in cancer treatment. *Nanomaterials (Basel, Switzerland)*, *9*(4), 638. https://doi.org/10.3390/nano9040638.

Gustafsson, J., Ljusberg-Wahren, H., Almgren, M., Larsson, K. (1996). Cubic lipid-water phase dispersed into submicron particles. *Langmuir*, 12, 4611–3.https://doi.org/10.1021/LA960318Y

Nasri, S., Ebrahimi-Hosseinzadeh, B., Rahaie, M., Sahraeian, R. (2020). Thymoquinone-loaded ethosome with breast cancer potential: Optimization, in vitro and biological assessment. *Journal Nanostructure Chemistry*, *10*, 19–31.

Kumbhar, P.S., Sakate, A.M., Patil, O.B., Manjappa, A. S., Disouza, J. I. (2020). Podophyllotoxin-polyacrylic acid conjugate micelles: improved anticancer efficacy against multidrug-resistant breast cancer. *Journal of Egyptian National Cancer Institute,* 32, 42, 1-8. https://doi.org/10.1186/s43046-020-00053-1.

Lakshmi, N. M., Yalavarthi, P. R., Vadlamudi, H. C., Thanniru, J., Yaga, G., K, H. (2014). Cubosomes as targeted drug delivery systems - a biopharmaceutical approach. *Current Drug Discovery Technologies*, *11*(3), 181–188. https://doi.org/10.2174/1570163811666140505125923.

McQuade, R. M., Stojanovska, V., Donald, E., Abalo, R., Bornstein, J. C., Nurgali, K. (2016). Gastrointestinal dysfunction and enteric neurotoxicity following treatment with anticancer chemotherapeutic agent 5-fluorouracil. *Neurogastroenterology and Motility: The Official Journal of the European Gastrointestinal Motility Society*, *28*(12), 1861–1875. https://doi.org/10.1111/nmo.12890

Nasr, M., Ghorab, M., Abdelazem, A. (2015). In vitro and in vivo evaluation of cubosomes containing 5-fluorouracil for liver targeting. *Acta Pharmaceutica B*, 5(1), 79–88.http://dx.doi.org/10.22159/ijap.2019v11i2.30582.

Noujaim, J., Constantinidou, A., Messiou, C., Thway, K., Miah, A., Benson, C., Judson, I.,Jones, R. L. (2018). Successful ifosfamide rechallenge in soft-tissue sarcoma. *American Journal of Clinical Oncology*, *41*(2), 147–151. https://doi.org/10.1097/COC.0000000000000243.

Rick D, Kellerman MD. (2021). In conn's current therapy. Elsevier, 1165-1168.

Saito, Y., Kumamoto, T., Makino, Y., Tamai, I., Ogawa, C., Terakado, H. (2016). A retrospective study of treatment and prophylaxis of ifosfamide-induced hemorrhagic cystitis in pediatric and adolescent and young adult (AYA) patients with solid tumors. *Japanese Journal of Clinical Oncology*, 46 (9), 856–861. https://doi.org/10.1093/jjco/hyw093.

Sambamoorthy, U., Manjappa, A. S., Eswara, B., Sanapala, A. K., Nagadeepthi, N. (2021). Vitamin E Oil Incorporated Liposomal Melphalan and Simvastatin: approach to obtain improved physicochemical characteristics of hydrolysable melphalan and anticancer activity in combination with simvastatin against multiple myeloma. *AAPS PharmSciTech*, *23*(1), 23. https://doi.org/10.1208/s12249-021-02177-6.

Siddiqui, J. F., Rizwana, I. (2019). UV-visible spectrophotometric method development and validation for the estimation of ifosfamide in bulk drug and pharmaceutical dosage form. *International Journal of Pharmaceutical Sciences Review and Research*, 59(1), 102-105.

Singh-Joy, S. D., McLain, V. C. (2008). Safety assessment of poloxamers 101, 105, 108, 122, 123, 124, 181, 182, 183, 184, 185, 188, 212, 215, 217, 231, 234, 235, 237, 238, 282, 284, 288, 331, 333, 334, 335, 338, 401, 402, 403, and 407, poloxamer 105 benzoate, and poloxamer 182 dibenzoate as used in cosmetics. *International Journal of Toxicology*, *27 Suppl 2*, 93–128. https://doi.org/10.1080/10915810802244595.

Suwankhong, D., Liamputtong, P. (2018). Physical and Emotional Experiences of Chemotherapy: A qualitative study among women with breast cancer in Southern Thailand. *Asian Pacific Journal of Cancer Prevention: APJCP*, *19*(2), 521–528. https://doi.org/10.22034/APJCP.2018.19.2.521

Wang, S. Q., Zhang, Q., Sun, C., Liu, G. Y. (2018). Ifosfamide-loaded lipid-core-nanocapsules to increase the anticancer efficacy in MG63 osteosarcoma cells. *Saudi Journal of Biological Sciences*, *25*(6), 1140–1145. https://doi.org/10.1016/j.sjbs.2016.12.001.

Zhang, J., Ng, K. Y., & Ho, P. C. (2010). Interaction of oxazaphosphorines with multidrug resistance-associated protein 4 (MRP4). *AAPS Journal*, *12*(3), 300–308. https://doi.org/10.1208/s12248-010-9189.